Clinical application of ultrashort echo time (UTE) and zero echo time (ZTE) magnetic resonance (MR) imaging in the evaluation of osteoarthritis

Karen Y. Cheng[1], **Dina Moazamian**[1], **Yajun Ma**[1], **Hyungseok Jang**[1], **Saeed Jerban**[1,2,3], **Jiang Du**[1,2,4], **Christine B. Chung**[1,5,*]

[1]Department of Radiology, University of California, San Diego

[2]Research Service, Veterans Affairs San Diego Healthcare System

[3]Department of Orthopedic Surgery, University of California, San Diego

[4]Department of Bioengineering, University of California, San Diego

[5]Department of Radiology, Veterans Affairs San Diego Healthcare System

Abstract

Novel compositional magnetic resonance (MR) imaging techniques have allowed for both the qualitative and quantitative assessment of tissue changes in osteoarthritis, many of which are difficult to characterize on conventional MR imaging. Ultrashort echo time (UTE) and zero echo time (ZTE) MR imaging has not been broadly implemented clinically but has several applications that leverage contrast mechanisms for morphologic evaluation of bone and soft tissue, as well as biochemical assessment in various stages of osteoarthritis progression. Many of the musculoskeletal tissues implicated in the initiation and progression of osteoarthritis are short T2 in nature, appearing dark as signal has already decayed to its minimum when image sampling starts. UTE and ZTE MR imaging allow for the qualitative and quantitative assessment of these short T2 tissues (bone, tendon, calcified cartilage, meniscus, ligament) with both structural and functional reference standards described in the literature[1–3]. This review will describe applications of UTE and ZTE MR imaging in musculoskeletal tissues focusing on its role in knee osteoarthritis. While the review will address tissue specific applications of these sequences, it is understood that osteoarthritis is a whole joint process with involvement and interdependence of all tissues.

Keywords

*Senior and corresponding author: Christine B. Chung, MD, cbchung@health.ucsd.edu, University of California, San Diego, Veterans Affairs Medical Center, San Diego, 9427 Health Sciences Drive, La Jolla, CA 92093, tel: (858)822-1333, fax: (858)822-1331, twitter: @CBChung_ucsd.

Introduction

Magnetic resonance (MR) imaging has become increasingly important for the detection and characterization of osteoarthritis, and particularly of knee osteoarthritis. With advances in technology, MR imaging offers morphologic assessment of musculoskeletal tissues through excellent soft tissue contrast, high-resolution and quantitative techniques. These capabilities have facilitated the ability to characterize the broad range of structural alteration that occurs in vastly different musculoskeletal tissues across the range of mild to severe degenerative osteoarthritis. Many of the tissues of interest in osteoarthritis—including menisci, ligaments, calcified cartilage, and subchondral bone—have very short T2 relaxation times related to their intrinsic structure. At the time image sampling starts with standard MR imaging sequences, signal has decayed to its minimum rendering short T2 tissues "invisible" or opaque to detection of structural change through standard diagnostic methods of identification of signal alteration. UTE and ZTE imaging have emerged as techniques to enable both visual and quantitative assessment of these short T2 tissues. UTE imaging uses echo times (TE) that are 100 μs or less, at least 20–50-fold shorter than the shortest conventional MR imaging echo times, which are on the order of several milliseconds. ZTE imaging is an extension of this approach which enables signal acquisition immediately after the application of the radiofrequency pulse at near-zero TE. These techniques allow for the detection of signal from tissues with very short T2 relaxation times before the signal has decayed.

UTE and ZTE imaging of tissues in osteoarthritis

Calcified Cartilage and Osteochondral Junction

Normal articular cartilage has a layered architecture, with the collagen fibrils that provide scaffolding for cartilage structure anchored in the subjacent subchondral bone. The deepest layer of cartilage is calcified and interdigitates with the subchondral bone, providing a structural and material property transition of intermediate stiffness between the overlying uncalcified radial zone cartilage and the underlying subchondral bone that helps resist delamination due to shear force [4]. The thickness of this calcified zone of cartilage has been shown to decrease with increasing age [5]. In addition, alterations in the thickness of the zone of calcified cartilage and subchondral bone plate are thought to be associated with osteoarthritis and chondral damage[6,7]. Further, proteoglycan synthesis in the zone of calcified cartilage has been shown to occur within cartilage in response to subfracture impaction injuries in the absence of chondral surface disruption [8].These findings suggest that the chondral abnormalities associated with osteoarthritis may not progress from damage beginning at the superficial layer and extending deeper with greater severity of injury as has been classically described (e.g. "outside-in"), but may instead begin with insults to the deep cartilage structures and only propagate to more superficial structures later (e.g. "inside-out"). Moreover, they highlight the importance of assessing these deep structures of cartilage.

As a result of its higher proportion of hydroxyapatite, higher density of collagen fibrils, and lower water content compared to the uncalcified cartilage, the layer of calcified cartilage has a shorter T2 relaxation time (ranging from 1 to 3.3 ms) and may be indistinguishable from the underlying subchondral bone (less than 1 ms) on conventional MR imaging, as

signals from both tissues have decayed by the time of image acquisition [4,9,10]. The application of UTE MR imaging in the knee was introduced more than 20 years ago by several investigators [11,12]. With technical advances in UTE MR imaging, contrast mechanisms were optimized to provide facile identification and characterization of these short T2 tissues, with the normal appearance of the calcified zone of cartilage represented by linear high signal intensity at the subchondral bone interface[13,14]. In osteoarthritis, the osteochondral junction may be abnormal, with qualitative disruption in the normal high signal intensity band (Figure 1) [15], perhaps even before there are conventional imaging features consistent with osteoarthritis[16]. Additional morphologic changes on UTE MR imaging sequences of the calcified cartilage include effacement or widening of its normal bright signal[15–17]. Subsequent work has developed 3D UTE sequences to reduce partial-volume effects, including a 3D adiabatic inversion recovery prepared (IR) UTE Cones sequence [15] and more recently a 3D dual IR UTE Cones sequence[18], which have enabled the application of these techniques *in vivo*. Mackay, et al., applied 3D UTE MR imaging in a small cohort of patients with knee pain and found that those with pain had changes in the morphologic appearance of the calcified layer of cartilage with associated regions of increased T2 values in superficial cartilage, reinforcing the importance of the calcified cartilage in the development of osteoarthritis [16]. Further technical development has focused on high resolution, high contrast imaging with fast UTE MR imaging scan times on the order of 3 minutes, increasing the practicality of inclusion of these sequences into standard osteoarthritis protocols[19].

Quantitative imaging of the calcified layer of cartilage has been studied using UTE MR imaging for evaluation of T2* and T1 rho mapping, the former assessing collagen content and orientation and the latter proteoglycan content. As previously noted, T2* values in the calcified cartilage were found to range from 1.0 to 3.3 ms, with T1 rho values from 2.2 to 4.6 ms [10]. In a study of subjects after ACL injury, UTE T2* values in a cohort with intact cartilage were shown to discriminate between uninjured controls and subjects with Outerbridge grade 0 and 1 cartilage classification. In addition, UTE T2* values were shown to normalize with longitudinal assessment in treated subjects, establishing the ability to identify calcified cartilage injury as well as track response to therapy, both crucial to identifying initiating steps in osteoarthritis [20]. UTE T2* values have also been shown to be elevated with increased varus alignment of the knee, as well as increased knee adduction moment, both known clinical markers of increased risk for osteoarthritis [21]. Recently, UTE MR imaging has been used in conjunction with T1, T1 rho, macromolecular fraction (MMF), and T2* for evaluation of the osteochondral junction in cadaveric knees. Results indicated that T1, T1 rho and T2* relaxation times increased from deep to superifical cartilage, whereas MMF decreased from the osteochondral junction to superficial cartilage. Higher grades of cartilage degeneration by MR grading systems correlated with increased T1, T1 rho and T2* values (Figure 2), while the MMF was negatively correlated with grade of chondral degeneration [22]. These findings speak to the ability of UTE MR imaging to assess compositional features of the calcified layer of cartilage and interrogate its role in early osteoarthritis.

Meniscus

Meniscal integrity is key and crucial to overall knee joint health with meniscal pathology having a central role in structural progression of knee osteoarthritis[23]. UTE MR imaging has been leveraged to directly visualize the fibrillar infrastructure of the meniscus in ex vivo meniscal samples, establishing the foundation for application of quantitative UTE MR imaging techniques[24]. Quantitative UTE MR imaging has been applied to meniscal evaluation in both ex vivo human meniscal tissue and patient cohorts. UTE T2* values have been shown to distinguish degenerated and torn menisci from normal, with higher T2* values in torn menisci than with degeneration (Figure 3)[25,26]. Further, and perhaps most compelling, one study demonstrated not only the potential for UTE T2* mapping to identify occult, subclinical meniscal injury, but to follow response to therapy[20]. In this study of 42 patients who underwent ACL reconstruction, UTE T2* values were increased, even when the meniscus was confirmed to be normal at arthroscopy. This is not surprising as arthroscopic evaluation is confined to surface evaluation of the meniscus, without the ability to interrogate its infrastructure. Meniscus damage, particularly involving the posterior horn of the lateral meniscus, is common in the setting of ACL injury and has been associated with meniscus extrusion, which increases the risk of knee osteoarthritis due to greater exposure of the tibial cartilage and reduced ability to disperse load and absorb shock. Even after ACL reconstruction, approximately 50–70% of patients develop osteoarthritis within 10–15 years after their initial injury underlining the importance for a method to non-invasively assess structural alterations in tissues such as the meniscus[27].

Though UTE MR imaging techniques for meniscal evaluation have largely focused on T2* quantification, other techniques have been applied and include T1 rho and UTE MR imaging with magnetization transfer modeling (UTE-MT) for calculation of macromolecular fraction (MMF). T1 rho techniques have been deployed for meniscal evaluation (Figure 4), but to a much lesser degree than in cartilage. This may be partly due to the lower concentration of proteoglycan in meniscus (1–2%) compared to hyaline articular cartilage (5–10%). While T1 rho MR imaging has shown altered values in the menisci consistent with degeneration in ACL-injured patients, the UTE T1 rho sequence has not been broadly used for meniscal evaluation[28]. UTE T1 rho imaging of the meniscus has been performed in cadaveric donor tissue as well as healthy volunteers to assess meniscal proteoglycan content [29]. The UTE T1 rho sequence has also been highlighted as an imaging marker of tissue function in the setting of meniscal loading with the ability to detect deformation patterns. In a study in cadaveric knee donor tissue, the UTE T1 rho sequence showed altered values in the loaded knee, with partial restoration of the UTE T1 rho value with unloading[30]. MMF, as the main parameter calculated by UTE-MT modeling, estimates macromolecular matrix density (collagen and proteoglycan) in meniscus. With compression of meniscal tissue, outward water flux occurs with a subsequent increase in MMF. In a study using young and elderly cadaveric donor tissue with varying degrees of degeneration, MMF calculation with UTE-MT techniques highlighted the potential of the technique to noninvasively characterize effects of tissue deformation with knee loading[31]. Though these techniques have not been broadly used in cohorts with osteoarthritis, the ability to interrogate proteoglycan content and functional change in the meniscus are compelling tools to detect early meniscal degeneration.

Chondrocalcinosis

Chondrocalcinosis or calcium pyrophosphate crystal deposition (CPPD) has been associated with osteoarthritis, though it is not clear whether it is the result of a systemic process that leads to osteoarthritis, it predisposes to or results from osteoarthritis[32]. The prevalence of CPPD is estimated to be 4–7% and it is considered a disease of aging[33]. In a recent study assessing a calcium-containing crystal cohort from the Osteoarthritis Initiative, crystal deposition was associated with increased cartilage and meniscal degeneration over a four-year period. The study suggested that an assessment of the crystal burden may be useful to evaluate risk of onset and worsening of degenerative disease[34]. Imaging methods used for detection of calcifications in articular cartilage and menisci have been x-ray-based, focusing on the conventional radiographs and computed tomography (CT) [32]. In the ACR/EULAR consensus criteria for CPPD diagnosis, MR imaging has not been recommended for the assessment of CPPD as it has relatively low specificity and historically poor spatial resolution as compared to other techniques such as CT [35,36]. The MR imaging literature has described limited use of gradient-echo sequences and DESS (dual echo steady state) with some success, the latter at 3T and 7T, for the detection of chondrocalcinosis using CT as a reference standard. In these studies, chondral calcifications appear low in signal intensity on the background of higher signal normal hyaline cartilage. It has been suggested that 7T MR imaging may offer significantly higher sensitivity in detection of chondral calcific deposits compared to 3T MR imaging in patient populations[33]. MR imaging of calcifications in meniscus has been more challenging, even at ultra-high field strength, due to the short T2 nature of both the meniscal tissue and calcifications with similar contrast on standard MR imaging sequences. UTE MR imaging techniques enable direct visualization of meniscal calcification[37]. On UTE MR images, CPPD appears as punctate dark regions within the menisci (Figure 5). Interestingly, on a study of nine cadaveric knees, calcium pyrophosphate deposits were almost exclusively found in the central avascular zones of the meniscus[32]. Not surprisingly, compared to normal tissue, menisci with crystal deposition had higher indentation stiffness [32].

Osseous structures and Zero Echo Time Imaging

The hallmarks of osteoarthritis include joint space narrowing, osteophytosis and subchondral trabecular remodeling resulting in sclerosis. These findings have historically been characterized on radiographs or CT, focusing on implementation of MR imaging for soft tissue evaluation[38]. Interest in MR imaging sequences with CT-like contrast has increased for many reasons, including consideration of ALARA (As Low As Reasonably Acceptable) principles for radiation exposure, healthcare cost and efficiency of health care delivery [39,40].

Cortical and trabecular bone have very short T2 values (less than 0.5 ms) making MR imaging extremely challenging. Several techniques have been used to create "CT-like" contrast with MR imaging. These include UTE, ZTE, and gradient echo (GRE) sequences. ZTE MR imaging has the broadest clinical deployment for synthetic CT to date and allows for direct visualization of the cortical bone. This sequence can generate tissue contrast similar to CT, with isotropic or near-isotropic acquisitions with resolution of 0.8 −1.2 mm, only slightly greater than the 0.625 mm resolution of CT[41]. ZTE has already been applied

in numerous clinical settings that previously required CT imaging such as the evaluation of craniofacial abnormalities [42] and glenoid bone stock [43]. With regard to degenerative changes, ZTE has been shown to be comparable to CT in the assessment of sacroiliac joint [39] and lumbar spine [44]. In the lumbar spine, ZTE was more sensitive to cortical bone abnormalities and osteophytes compared to conventional MR imaging [44]. Similarly, applying ZTE to imaging of knee osteoarthritis will likely allow for improved detection of small osteophytes in the setting of early osteoarthritis detectable on MR imaging (Figure 6). With broad adoption of MR imaging with CT-like contrast as an acceptable surrogate for osseous evaluation, diagnostic imaging algorithms as we currently know them will undergo significant transformation due to the ability of MR imaging to provide a one-stop-shop for soft tissue and bone evaluation.

Quantitative Hemosiderin

There has been increasing recognition that inflammatory pathways play an important role in the development of osteoarthritis, with both the synovium and infrapatellar (Hoffa's) fat pad containing cells that secrete inflammatory cytokines, interleukins, growth factors, and adipokines that may regulate cartilage protein production [45]. In hemophilia, as well as in non-hemophilic hemosiderotic synovitis, recurrent intra-articular hemorrhage results in intracellular hemosiderin deposition in these tissues which can trigger in a release of pro-inflammatory cytokines that contribute to cartilage destruction[46,47]. UTE quantitative susceptibility mapping (UTE-QSM) is a technique that has been shown to be feasible in non-invasively quantitating the amount of hemosiderin within the knee (or ankle) joint in hemophilic patients (Figure 7) [48]. Healthy volunteers in this study exhibited no regions of high susceptibility to indicate significant hemosiderin staining. Hemosiderin deposition has also been noted in other conditions such as infrapatellar fat pad impingement (Hoffa disease)[49,50], and it is conceivable that the hemosiderin in such cases may be a precursor to chondral loss and osteoarthritis. Future application of this technique in the imaging of patients with osteoarthritis or at risk for osteoarthritis may be able to detect more modest quantities of hemosiderin deposition, intermediate between those of healthy and hemophilic patients, providing a quantitative measure of synovial or Hoffa's fat pad iron content which may be associated with accelerated chondral degeneration.

Conclusions

UTE and ZTE MR imaging are accurate, non-invasive means to assess various tissues in the knee joint for early degenerative change. They allow for the acquisition of signal from structures that would otherwise have no detectable signal at conventional MR, enabling the radiologist to evaluate for subclinical injuries that may predispose the patient to osteoarthritis, potentially allowing for earlier intervention and treatment to avoid progression to osteoarthritis. In addition, ZTE MR imaging generates images with CT-like contrast such that future diagnostic imaging algorithms may utilize a single MR imaging scan for assessment of both soft tissue and osseous structures.

Funding

References

[1]. Baum T, Joseph GB, Karampinos DC, Jungmann PM, Link TM, Bauer JS. Cartilage and meniscal T2 relaxation time as non-invasive biomarker for knee osteoarthritis and cartilage repair procedures. Osteoarthritis Cartilage 2013;21:1474–84. 10.1016/j.joca.2013.07.012. [PubMed: 23896316]

[2]. Dunn TC, Lu Y, Jin H, Ries MD, Majumdar S. T2 Relaxation Time of Cartilage at MR Imaging: Comparison with Severity of Knee Osteoarthritis. Radiology 2004;232:592–8. 10.1148/radiol.2322030976. [PubMed: 15215540]

[3]. Rauscher I, Stahl R, Cheng J, Li X, Huber MB, Luke A, et al. Meniscal Measurements of T1ρ and T2 at MR Imaging in Healthy Subjects and Patients with Osteoarthritis. Radiology 2008;249:591–600. 10.1148/radiol.2492071870. [PubMed: 18936315]

[4]. Bae WC, Biswas R, Chen K, Chang EY, Chung CB. UTE MRI of the Osteochondral Junction. Curr Radiol Rep 2014;2:35. 10.1007/s40134-013-0035-7. [PubMed: 25061547]

[5]. Lane L, Bullough P. Age-related changes in the thickness of the calcified zone and the number of tidemarks in adult human articular cartilage. J Bone Joint Surg Br 1980;62-B:372–5. 10.1302/0301-620X.62B3.7410471.

[6]. Oegema TR, Carpenter RJ, Hofmeister F, Thompson RC. The interaction of the zone of calcified cartilage and subchondral bone in osteoarthritis. Microsc Res Tech 1997;37:324–32. 10.1002/(SICI)1097-0029(19970515)37:4<324::AID-JEMT7>3.0.CO;2-K. [PubMed: 9185154]

[7]. Radin EL, Burr DB, Caterson B, Fyhrie D, Brown TD, Boyd RD. Mechanical determinants of osteoarthrosis. Semin Arthritis Rheum 1991;21:12–21. 10.1016/0049-0172(91)90036-Y.

[8]. Donohue JM, Buss D, Oegema TRJ, Thompson RCJ. The effects of indirect blunt trauma on adult canine articular cartilage. JBJS 1983;65:948–57.

[9]. Mahar R, Batool S, Badar F, Xia Y. Quantitative measurement of T2, T1ρ and T1 relaxation times in articular cartilage and cartilage-bone interface by SE and UTE imaging at microscopic resolution. J Magn Reson 2018;297:76–85. 10.1016/j.jmr.2018.10.008. [PubMed: 30366222]

[10]. Du J, Carl M, Bae WC, Statum S, Chang E, Bydder GM, et al. Dual Inversion Recovery Ultrashort Echo Time (DIR-UTE) Imaging and Quantification of the Zone of Calcified Cartilage (ZCC). Osteoarthr Cartil OARS Osteoarthr Res Soc 2013;21:77–85. 10.1016/j.joca.2012.09.009.

[11]. Brossmann J, Frank LR, Pauly JM, Boutin RD, Pedowitz RA, Haghighi P, et al. Short echo time projection reconstruction MR imaging of cartilage: comparison with fat-suppressed spoiled GRASS and magnetization transfer contrast MR imaging. Radiology 1997;203:501–7. 10.1148/radiology.203.2.9114112. [PubMed: 9114112]

[12]. Gold GE, Thedens DR, Pauly JM, Fechner KP, Bergman G, Beaulieu CF, et al. MR imaging of articular cartilage of the knee: new methods using ultrashort TEs. Am J Roentgenol 1998;170:1223–6. 10.2214/ajr.170.5.9574589. [PubMed: 9574589]

[13]. Shao H, Chang EY, Pauli C, Zanganeh S, Bae W, Chung CB, et al. UTE bi-component analysis of T2* relaxation in articular cartilage. Osteoarthritis Cartilage 2016;24:364–73. 10.1016/j.joca.2015.08.017. [PubMed: 26382110]

[14]. Du J, Takahashi AM, Bae WC, Chung CB, Bydder GM. Dual inversion recovery, ultrashort echo time (DIR UTE) imaging: Creating high contrast for short-T2 species. Magn Reson Med 2010;63:447–55. 10.1002/mrm.22257. [PubMed: 20099332]

[15]. Ma Y-J, Jerban S, Carl M, Wan L, Guo T, Jang H, et al. Imaging of the region of the osteochondral junction (OCJ) using a 3D adiabatic inversion recovery prepared ultrashort echo time cones (3D IR-UTE-cones) sequence at 3 T. NMR Biomed 2019;32:e4080. 10.1002/nbm.4080. [PubMed: 30794338]

[16]. Mackay JW, Low SBL, Houston GC, Toms AP. Ultrashort TE evaluation of the osteochondral junction in vivo: a feasibility study. Br J Radiol 2016;89:20150493. 10.1259/bjr.20150493. [PubMed: 26781345]

[17]. Bae WC, Dwek JR, Znamirowski R, Statum SM, Hermida JC, D'Lima DD, et al. Ultrashort Echo Time MR Imaging of Osteochondral Junction of the Knee at 3 T: Identification of Anatomic Structures Contributing to Signal Intensity1. Radiology 2010;254:837–45. 10.1148/radiol.09081743. [PubMed: 20177096]

[18]. Lombardi AF, Jang H, Wei Z, Jerban S, Wallace M, Masuda K, et al. High-contrast osteochondral junction imaging using a 3D dual adiabatic inversion recovery-prepared ultrashort echo time cones sequence. NMR Biomed 2021;34:e4559. 10.1002/nbm.4559. [PubMed: 34021649]

[19]. Cai Z, Wei Z, Wu M, Jerban S, Jang H, Li S, et al. Knee Osteochondral Junction Imaging Using a Fast 3D T1-weighted Ultrashort Echo Time Cones Sequence at 3T. Magn Reson Imaging 2020;73:76–83. 10.1016/j.mri.2020.08.003. [PubMed: 32828984]

[20]. Chu CR, Williams AA, West RV, Qian Y, Fu FH, Do BH, et al. Quantitative Magnetic Resonance Imaging UTE-T2* Mapping of Cartilage and Meniscus Healing After Anatomic Anterior Cruciate Ligament Reconstruction. Am J Sports Med 2014;42:1847–56. 10.1177/0363546514532227. [PubMed: 24812196]

[21]. Titchenal MR, Williams AA, Chehab EF, Asay JL, Dragoo JL, Gold GE, et al. Cartilage Subsurface Changes to Magnetic Resonance Imaging UTE-T2* 2 Years After Anterior Cruciate Ligament Reconstruction Correlate With Walking Mechanics Associated With Knee Osteoarthritis. Am J Sports Med 2018;46:565–72. 10.1177/0363546517743969. [PubMed: 29293364]

[22]. Lombardi AF, Moazamian D, Jerban S, Jang H, Le N, Chung CB, et al. Quantitative Ultrashort Echo Time (UTE) Imaging of Osteochondral Junction [Abstract]. Int. Magn. Reson. Med, 2022.

[23]. Englund M, Roemer FW, Hayashi D, Crema MD, Guermazi A. Meniscus pathology, osteoarthritis and the treatment controversy. Nat Rev Rheumatol 2012;8:412–9. 10.1038/nrrheum.2012.69. [PubMed: 22614907]

[24]. Bae WC, Du J, Bydder GM, Chung CB. Conventional and Ultrashort MRI of Articular Cartilage, Meniscus and Intervertebral Disc. Top Magn Reson Imaging TMRI 2010;21:275–89. 10.1097/RMR.0b013e31823ccebc. [PubMed: 22129641]

[25]. Bae WC, Tadros AS, Finkenstaedt T, Du J, Statum S, Chung CB. Quantitative magnetic resonance imaging of meniscal pathology ex vivo. Skeletal Radiol 2021;50:2405–14. 10.1007/s00256-021-03808-6. [PubMed: 33983499]

[26]. Juras V, Apprich S, Zbý Š, Zak L, Deligianni X, Szomolanyi P, et al. Quantitative MRI analysis of menisci using biexponential T2* fitting with a variable echo time sequence. Magn Reson Med 2014;71:1015–23. 10.1002/mrm.24760. [PubMed: 23606167]

[27]. Wang A, Pedoia V, Su F, Abramson E, Kretzschmar M, Nardo L, et al. MR T1ρ and T2 of meniscus after acute anterior cruciate ligament injuries. Osteoarthritis Cartilage 2016;24:631–9. 10.1016/j.joca.2015.11.012. [PubMed: 26620091]

[28]. Wang L, Chang G, Bencardino J, Babb JS, Rokito A, Jazrawi L, et al. T1rho MRI at 3T of menisci in patients with acute anterior cruciate ligament (ACL) injury. J Magn Reson Imaging 2015;41:544–9. 10.1002/jmri.24594. [PubMed: 24616029]

[29]. Du J, Carl M, Diaz E, Takahashi A, Han E, Szeverenyi NM, et al. Ultrashort TE T1rho (UTE T1rho) imaging of the Achilles tendon and meniscus. Magn Reson Med 2010;64:834–42. 10.1002/mrm.22474. [PubMed: 20535810]

[30]. Jerban S, Ma Y, Kasibhatla A, Wu M, Szeverenyi N, Guma M, et al. Ultrashort echo time adiabatic T1ρ (UTE-Adiab-T1ρ) is sensitive to human cadaveric knee joint deformation induced by mechanical loading and unloading. Magn Reson Imaging 2021;80:98–105. 10.1016/j.mri.2021.04.014. [PubMed: 33945858]

[31]. Jerban S, Kasibhatla A, Ma Y, Wu M, Chen Y, Guo T, et al. Detecting Articular Cartilage and Meniscus Deformation Effects Using Magnetization Transfer Ultrashort Echo Time (MT-UTE) Modeling during Mechanical Load Application: Ex Vivo Feasibility Study. CARTILAGE 2021;13:665S–673S. 10.1177/1947603520976771. [PubMed: 33289401]

[32]. Finkenstaedt T, Biswas R, Abeydeera NA, Siriwananrangsun P, Healey R, Statum S, et al. Ultrashort Time to Echo (UTE) MR Evaluation of Calcium Pyrophosphate Crystal Deposition (CPPD) in Human Menisci. Invest Radiol 2019;54:349–55. 10.1097/RLI.0000000000000547. [PubMed: 30688685]

[33]. Germann C, Galley J, Falkowski AL, Fucentese SF, Pfirrmann CWA, Nanz D, et al. Ultra-high resolution 3D MRI for chondrocalcinosis detection in the knee—a prospective diagnostic accuracy study comparing 7-tesla and 3-tesla MRI with CT. Eur Radiol 2021;31:9436–45. 10.1007/s00330-021-08062-x. [PubMed: 34047850]

[34]. Foreman SC, Gersing AS, von Schacky CE, Joseph GB, Neumann J, Lane NE, et al. Chondrocalcinosis is Associated with Increased Knee Joint Degeneration Over 4 Years: Data from the Osteoarthritis Initiative. Osteoarthritis Cartilage 2020;28:201–7. 10.1016/j.joca.2019.10.003. [PubMed: 31629813]

[35]. Tedeschi SK, Becce F, Pascart T, Guermazi A, Budzik J-F, Dalbeth N, et al. Imaging features of calcium pyrophosphate deposition (CPPD) disease: consensus definitions from an international multidisciplinary working group. Arthritis Care Res n.d.;n/a. 10.1002/acr.24898.

[36]. Bernabei I, Sayous Y, Raja AY, Amma MR, Viry A, Steinmetz S, et al. Multi-energy photon-counting computed tomography versus other clinical imaging techniques for the identification of articular calcium crystal deposition. Rheumatology 2021;60:2483–5. 10.1093/rheumatology/keab125. [PubMed: 33560293]

[37]. Omoumi P, Bae WC, Du J, Diaz E, Statum S, Bydder GM, et al. Meniscal Calcifications: Morphologic and Quantitative Evaluation by using 2D Inversion-Recovery Ultrashort Echo Time and 3D Ultrashort Echo Time 3.0-T MR Imaging Techniques—Feasibility Study. Radiology 2012;264:260–8. 10.1148/radiol.12111439. [PubMed: 22723564]

[38]. Samuel AJ, Kanimozhi D. Outcome measures used in patient with knee osteoarthritis: With special importance on functional outcome measures. Int J Health Sci 2019;13:52–60.

[39]. Wolharn L, Guggenberger R, Higashigaito K, Sartoretti T, Winklhofer S, Chung CB, et al. Detailed bone assessment of the sacroiliac joint in a prospective imaging study: comparison between computed tomography, zero echo time, and black bone magnetic resonance imaging. Skeletal Radiol 2022. 10.1007/s00256-022-04097-3.

[40]. Breighner RE, Bogner EA, Lee SC, Koff MF, Potter HG. Evaluation of Osseous Morphology of the Hip Using Zero Echo Time Magnetic Resonance Imaging. Am J Sports Med 2019;47:3460–8. 10.1177/0363546519878170. [PubMed: 31633993]

[41]. Aydıngöz Ü, Yıldız AE, Ergen FB. Zero Echo Time Musculoskeletal MRI: Technique, Optimization, Applications, and Pitfalls. RadioGraphics 2022:220029. 10.1148/rg.220029.

[42]. Lu A, Gorny KR, Ho M-L. Zero TE MRI for Craniofacial Bone Imaging. Am J Neuroradiol 2019;40:1562–6. 10.3174/ajnr.A6175. [PubMed: 31467238]

[43]. de Mello RAF, Ma Y, Ashir A, Jerban S, Hoenecke H, Carl M, et al. 3D Zero Echo Time (ZTE) MRI versus 3D CT for Glenoid Bone Assessment. Arthrosc J Arthrosc Relat Surg Off Publ Arthrosc Assoc N Am Int Arthrosc Assoc 2020;36:2391–400. 10.1016/j.arthro.2020.05.042.

[44]. Hou B, Liu C, Li Y, Xiong Y, Wang J, Zhang P, et al. Evaluation of the degenerative lumbar osseous morphology using zero echo time magnetic resonance imaging (ZTE-MRI). Eur Spine J 2022;31:792–800. 10.1007/s00586-021-07099-2. [PubMed: 35015138]

[45]. Clockaerts S, Bastiaansen-Jenniskens YM, Runhaar J, Van Osch GJVM, Van Offel JF, Verhaar JAN, et al. The infrapatellar fat pad should be considered as an active osteoarthritic joint tissue: a narrative review. Osteoarthritis Cartilage 2010;18:876–82. 10.1016/j.joca.2010.03.014. [PubMed: 20417297]

[46]. Jain VK, Singh RK, Kumar S, Netam SS, Jain SG, Shah PJ. Hemosiderotic synovitis: Highlighting the role of T2∗ weighted sequence in skeletal MRI. Egypt J Radiol Nucl Med 2016;47:1511–3. 10.1016/j.ejrnm.2016.08.010.

[47]. Bennett GL, Leeson MC, Michael A. Extensive hemosiderin deposition in the medial meniscus of a knee. Its possible relationship to degenerative joint disease. Clin Orthop 1988:182–5.

[48]. Jang H, von Drygalski A, Wong J, Zhou JY, Aguero P, Lu X, et al. Ultrashort Echo Time Quantitative Susceptibility Mapping (UTE-QSM) for Detection of Hemosiderin Deposition

in Hemophilic Arthropathy: a Feasibility Study. Magn Reson Med 2020;84:3246–55. 10.1002/mrm.28388. [PubMed: 32662904]

[49]. Jacobson JA, Lenchik L, Ruhoy MK, Schweitzer ME, Resnick D. MR imaging of the infrapatellar fat pad of Hoffa. RadioGraphics 1997;17:675–91. 10.1148/radiographics.17.3.9153705. [PubMed: 9153705]

[50]. Roemer FW, Jarraya M, Felson DT, Hayashi D, Crema MD, Loeuille D, et al. Magnetic resonance imaging of Hoffa's fat pad and relevance for osteoarthritis research: a narrative review. Osteoarthritis Cartilage 2016;24:383–97. 10.1016/j.joca.2015.09.018. [PubMed: 26455999]

Key Points

- UTE MR imaging allows for the qualitative and quantitative evaluation of short T2 tissues (bone, calcified cartilage, meniscus), enabling identification of both early degenerative changes and subclinical injuries that may predispose to osteoarthritis.

- ZTE MR imaging allows for the detection of signal from bone, which has some of the shortest T2 values, and generates tissue contrast similar to CT, potentially obviating the need for CT in the assessment of osseous features of osteoarthritis.
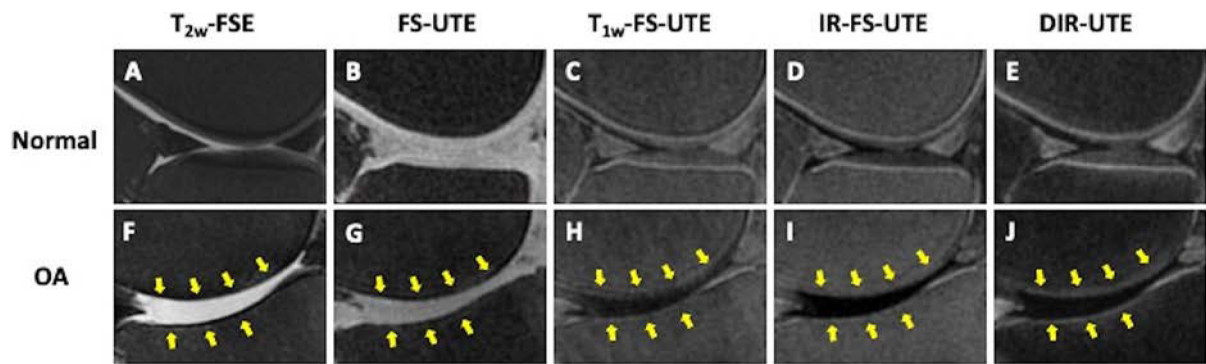
Figure 1.
High contrast 3D UTE osteochondral junction imaging in normal (A-E) and osteoarthritic (F-J) knees. In the normal knee, the osteochondral junction is hypointense on the clinical T2 FSE image (A) due to rapid signal decay but is hyperintense on the UTE images (B-E). In osteoarthritis, the hyperintense signal at the osteochondral junction is decreased on the UTE images (G-J, arrows) in the regions of chondral loss noted on conventional T2 FS image (F, arrows).
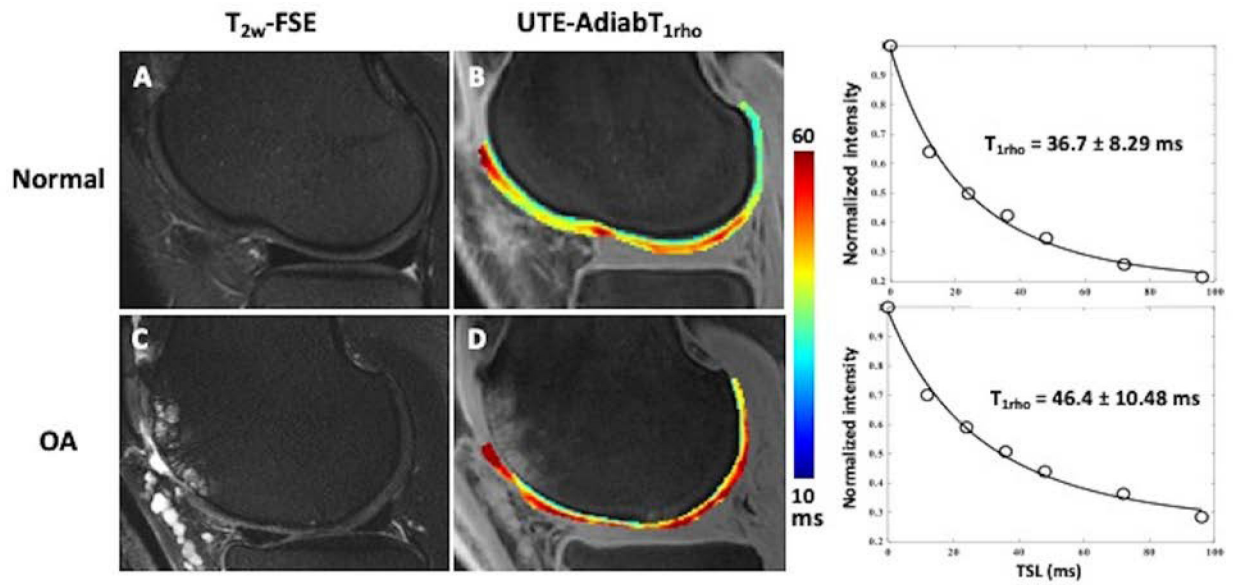
Figure 2.

In vivo 3D UTE-AdiabT$_{1rho}$ mapping of articular cartilage in normal (A-C) and osteoarthritic (D-F) knees. T$_{2w}$-FSE images demonstrates normal appearance of the cartilage in the normal knee (A) and diffuse chondral thinning with areas of high-grade chondral loss and subchondral cystic change in the osteoarthritic knee (D).The corresponding color maps (B, E) and UTE-AdibT1rho fitting curves (C, F) demonstrate elevated UTE-AdiabT$_{1rho}$ values in osteoarthritis (E, F) compared to the normal knee (B,C). Color map in both normal (B) and osteoarthritic (D) knees distinguish the calcified cartilage from superficial. Further the normal (B) color map demonstrates the zonal variation in T1 rho in the superficial cartilage.
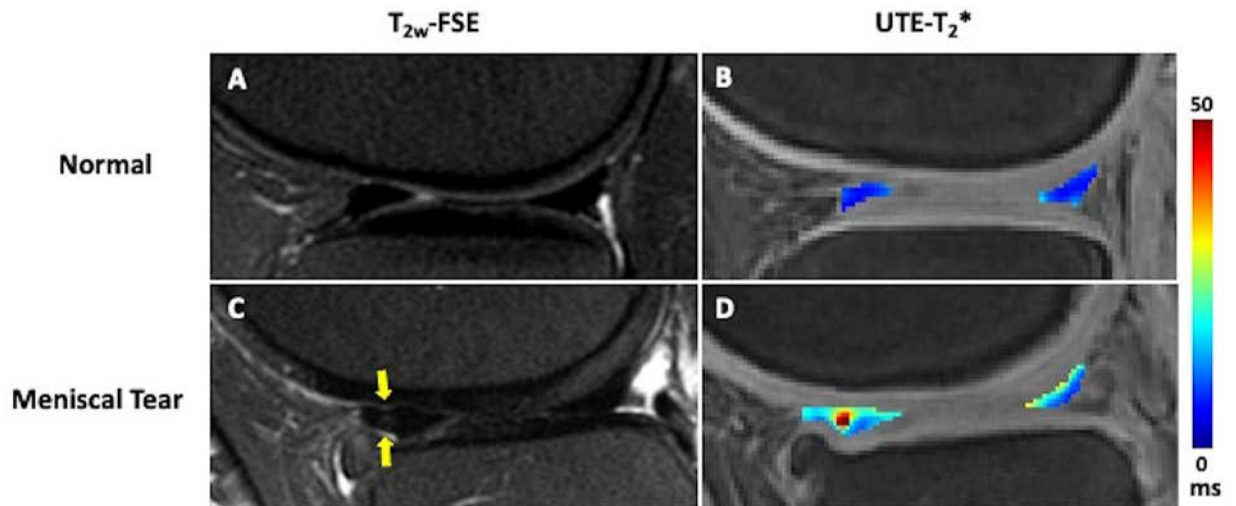
Figure 3.

In vivo 3D UTE-T_2* mapping of meniscus in a patient with intact menisci and normal cartilage (A,B) and a patient with osteoarthritis and a vertical tear of the anterior horn of the lateral meniscus (C,D). The meniscal UTE-T_2* values are elevated in the region of meniscal tear (D, indicated by arrows) compared to the intact meniscus (B). In addition, there is altered T2* in the posterior horn medial meniscus (D) which suggests meniscal degeneration. Deep to the torn anterior horn of the lateral meniscus, chondral loss is noted.
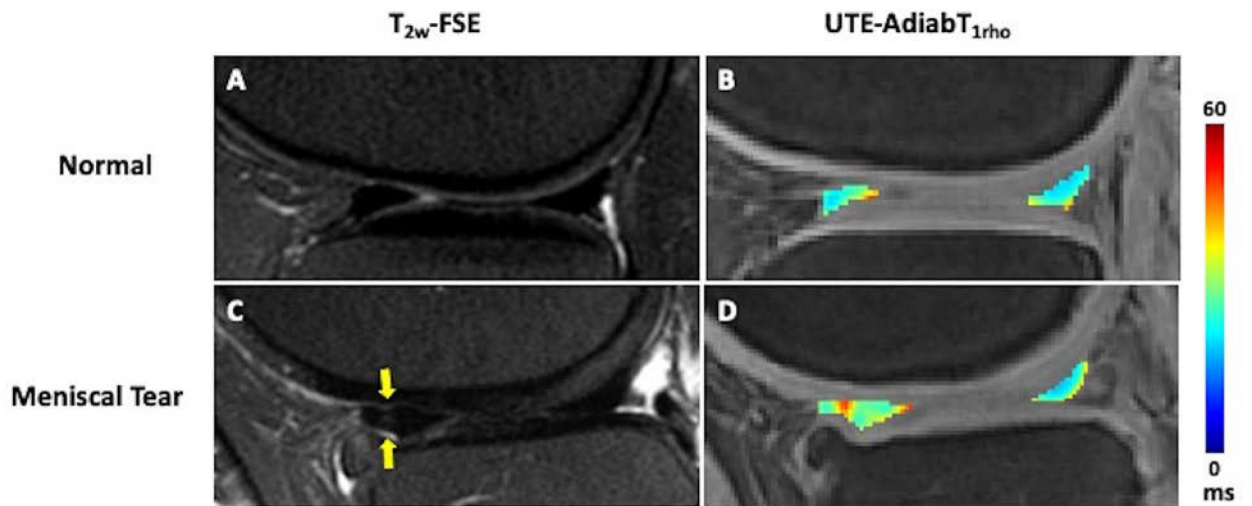
Figure 4.

In vivo 3D UTE-AdiabT$_{1rho}$ mapping of meniscus in a patient with normal cartilage and meniscus (A,B) and a patient with osteoarthritis and a vertical tear of the anterior horn of the lateral meniscus (B,C). The meniscal UTE-AdiabT$_{1rho}$ values are elevated in the region of meniscal tear (D, indicated by arrows) compared to the intact meniscus (B). Deep to the torn anterior horn of the lateral meniscus, chondral loss is noted.
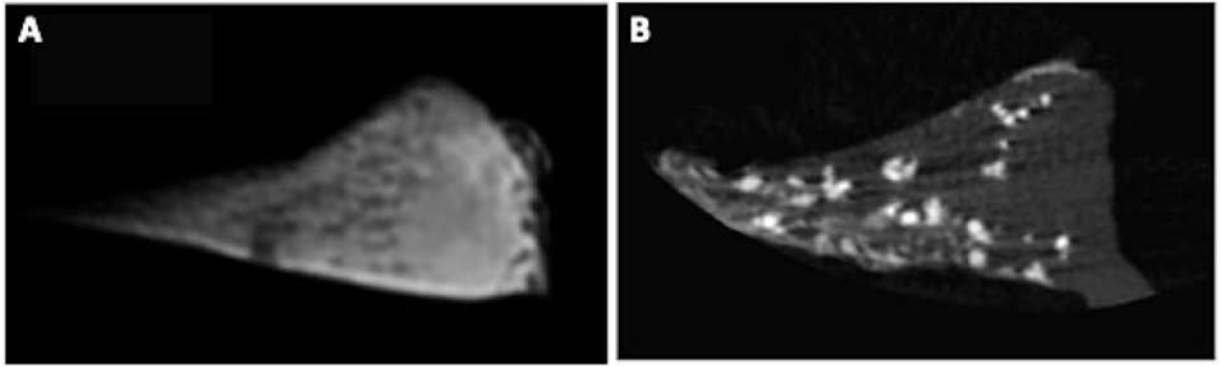
Figure 5.
UTE MR imaging (A) and micro CT (B) images of meniscal tissue with CPP deposits. On the UTE MR image (A), the meniscal tissue appears bright with punctate CPP deposits, which are confirmed on the micro CT (B) images.
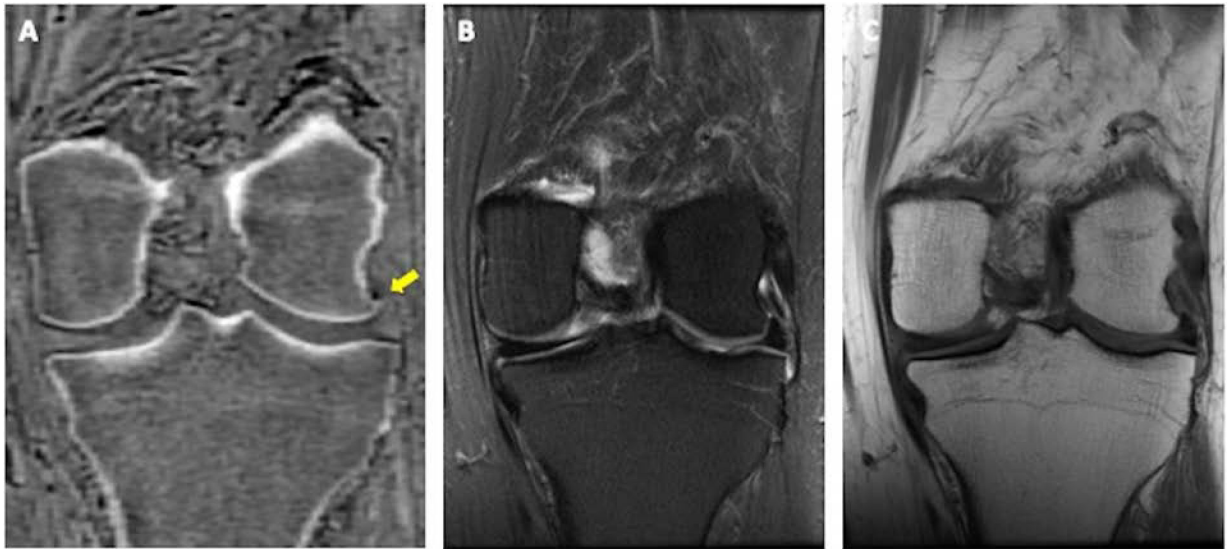
Figure 6.
CT-like contrast on coronal ZTE image (A, arrow) better displays a very small marginal osteophyte at the lateral femoral condyle as compared to conventional T2 FS (B) and T1(C) weighted images in this 58-year-old woman with chronic left knee pain.
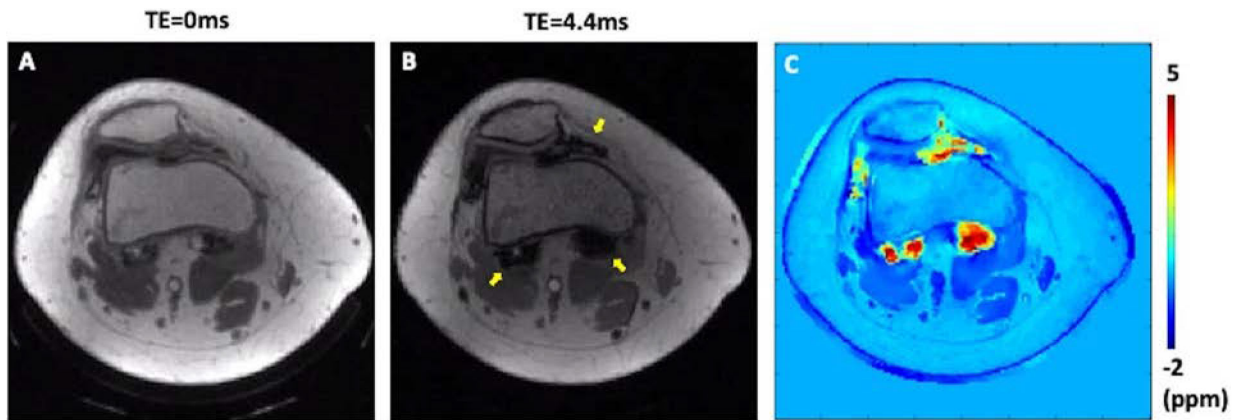
Figure 7.
UTE-QSM in a patient (28-year-old) with hemophilia type A. The patient had hemophilic arthropathy with a hemophilia joint health score (HJHS) of 12. Accumulated hemosiderin was observed in MRI, where UTE with TE of 0 ms (A) showed much reduced blooming artifacts compared to GRE with TE of 4.4ms (B, arrows). The resultant susceptibility map from UTE-QSM clearly detected the hemosiderin deposition and provided a quantitative assessment (C).